Available online at www.sciencedirect.com

SCIENCE DIRECT®

Cement and Concrete Research 35 (2005) 199–202

CEMENT AND CONCRETE RESEARCH

Density functional calculations of elastic properties of portlandite, $Ca(OH)_2$

J.L. Laugesen*

Department of Civil Engineering, Technical University of Denmark, Lyngby 2800, Denmark

Received 18 September 2003; accepted 19 July 2004

Abstract

The elastic constants of portlandite, $Ca(OH)_2$, are calculated by use of density functional theory. A lattice optimization of an infinite (periodic boundary conditions) lattice is performed on which strains are applied. The elastic constants are extracted by minimizing Hooke's law of linear elasticity, applying a least-square method. Young's modulus and bulk modulus are calculated from the stiffness matrix. The results are compared with the Brillouin zone spectroscopy results of F. Holuj et al. [F. Holuj, M. Drozdowski, M. Czajkowski, Brillouin spectrum of $Ca(OH)_2$, Solid State Commun., 56 (12) (1985) 1019–1021.]. An error estimate has been performed and the results are compared with experimental values.

PACS: 62.20.Dc

Keywords: Crystal structure; Elastic moduli; $Ca(OH)_2$; DFT

---

1. Introduction

The structure and elastic properties of portlandite, $Ca(OH)_2$, are of high importance in cement and concrete research. $Ca(OH)_2$ is one of the major phases in hydrated cement as it occupies 20–25% of the volume fraction of the total mass. Knowledge of the elastic properties is important in both experimental and theoretical modeling of cements on macro-, micro- and nanoscale modeling or any other scale. The presence of $Ca(OH)_2$ in cementitious materials influences mechanical properties such as strength, elasticity, cracking, shrinkage and creep.

Experimental determination of the elastic properties of portlandite may be undertaken by X-ray spectroscopy, however, this is difficult, since the crystals usually are too small. Alternatively, Brillouin zone spectroscopy may be used. This method is also considered to be more accurate, but requires more preparation of the sample. The present article concerns theoretical modeling of the elastic moduli. One similar calculation on portlandite has been reported [1], however, with another purpose than the determination of the elastic properties.

2. Principles of density functional theory

Density functional theory (DFT) provides a way to determine the total energy of a system as a functional of the electron density. For detailed information on DFT see the pioneer work of Hohenberg and Kohn [2] and Kohn and Sham [3]. An introduction to DFT has been written by Koch and Holthausen [4].

In this study, a plane wave pseudopotential software package, called DACAPO [5], has been used. In the plane wave pseudopotential approximation, the plane waves only describe the chemically active electrons (the valence electrons). The effects of the nucleus and the core electrons (the strongly bonded electrons) are replaced by a pseudopotential. Thus, the valence electrons are moving in a potential due to all nonchemically active charges. The basic problem is then to obtain a set of plane waves that describe the valence electrons in a given potential.

---

* Tel.: +45 45251774, +45 33258582.

E-mail address: jll@byg.dtu.dk.

0008-8846/$ - see front matter © 2004 Elsevier Ltd. All rights reserved.
doi:10.1016/j.cemconres.2004.07.036

The pseudopotentials used are generated by use of the generalized gradient approximation (GGA) developed by Perdew and Wang (PW91) [6]. These potentials are included in the software package. It should be noted that since the number of equations to solve grows by the cube of the number of electrons, it is extremely beneficial to apply pseudopotentials. To this may be added that, if a pseudopotential is not applied to describe the innermost electrons, a very large number of plane waves are often required due to fast variation of the nuclear potential, which further increases the computation times.

3. The crystal structure of portlandite

The crystal structure of portlandite is well known, and was found by X-ray spectroscopy by Bernal and Megaw in 1934 [7], Petch and Megaw in 1954 [8] and later by neutron diffraction by Busing and Levy in 1957 [9]. The morphology of the crystal is hexagonal and the crystal structure is trigonal with space group $P\bar{3}m1$. The lattice parameters is a=b=3.5930 Å, c=4.9090 Å, α=β=90° and γ=120°.

The trigonal unit cell shown in Fig. 1, contains five atoms. The Ca^{2+} ions are octahedrally coordinated by oxygen and each O^{2-} is tetrahedrally coordinated by calcium and one hydrogen. The structure is layered with the sheets lying in the (001) plane and with the octahedrals as building units. The oxygen and hydrogen all form hydroxyl groups with the direction perpendicular to the (001) plane. The smallest distance between hydrogen and oxygen across a layer is 2.757 Å and between pairs of oxygen atoms across the layer the smallest distance is 3.33 Å, thus, there will be no hydrogen bonds or other strong bonds across the layer. The layers mainly interact by weak dispersive forces.

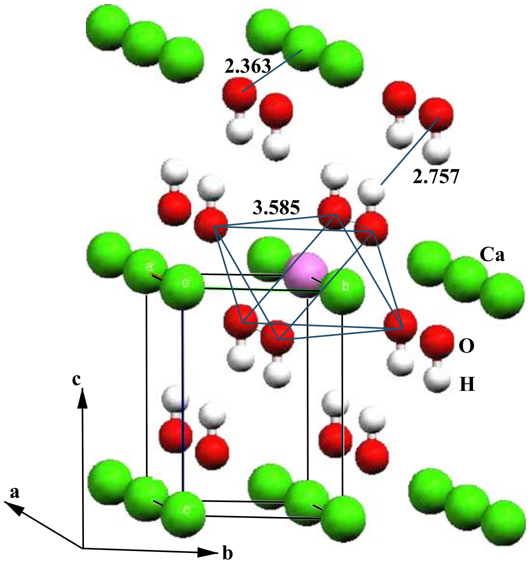

Fig. 1. The triclinic unit cell of portlandite. The coordination polyhedra show how the Ca^{2+} ion is coordinated by oxygen. These polyhedra are the building blocks of the layered structure.

4. Results

4.1. The calculated equilibrium states of portlandite

The equilibrium state of the system is very important for the correctness of stress–strain calculations. Firstly, due to the possibility of metastable states and secondly, due to the risk of being far from the region where the linearity of the elasticity holds.

The equilibrium state of portlandite has been calculated using a plane wave cutoff energy of 700 eV and 108 k-points within the first Brillouin zone generated from the Monkhorst–Pack scheme [10]. The k-points are equally distributed along the axes, with 6 k-points along each axis. The interaction between layers along the c-axis is very weak. It has been demonstrated by Baranek et al. [1], that the energy minimum depends highly on the spin polarization of the interaction between the layers, hence the calculation is performed spin polarized.

The relaxation of the system is performed iteratively, such that the relaxation alternates between an ionic relaxation and a lattice parameter relaxation. Each ionic relaxation is performed such that the maximum force on the atoms is below 0.01 eV/Å. The lattice parameters are relaxed to a state where the maximum residual stress component is lower than 3.10^{-4} eV/Å^4. In this way, the lattice parameters are calculated to be a=b=3.609 Å, c=4.864 Å. Compared to the X-ray diffraction results of Petch et al., this is a deviation of 0.5% on the a- and b-axes and 1% on the c-axis. Compared to the DFT/GGA calculation by Baranek et al. [1] there is only a difference in of 0.2% and 0.08% on the a- and b-axes, respectively.

4.2. Stress–strain calculations

The applied strains are all pure uniaxial or pure shear, meaning that only one of the strain components are nonzero and the strain tensor is symmetric. In this way, a whole column of the stiffness matrix may, in principle, be calculated with only one nonzero strain component. However, the uniaxial stresses are not independent from the off-diagonal components and a least-square method is used to fit the linear dependence. It may be shown [11] that a trigonal lattice in crystal class $\bar{3}m$ has six independent stiffness components forming the stiffness matrix

$$C_{i,j}=\begin{pmatrix} c_{11} & c_{12} & c_{13} & c_{14} & 0 & 0 \\ c_{12} & c_{11} & c_{13} & -c_{14} & 0 & 0 \\ c_{13} & c_{13} & c_{33} & 0 & 0 & 0 \\ c_{14} & -c_{14} & 0 & c_{44} & 0 & 0 \\ 0 & 0 & 0 & 0 & c_{44} & |c_{14}| \\ 0 & 0 & 0 & 0 & |c_{14}| & \frac{1}{2}(c_{11}-c_{12}) \end{pmatrix} \tag{1}$$

Table 1
The six elastic constants and Voigt and Reuss bounds for the bulk modulus of portlandite, all in units of GPa

	This work	Holuj et al. [12]	$\Delta/c \cdot 100\%$
c_{11}	99.39	99.28	0.11
c_{33}	36.29	32.60	10.2
c_{44}	7.88	9.846	25.0
c_{12}	30.78	36.21	17.6
c_{13}	7.36	29.65	303.0
c_{66}	34.31	31.55	8.0
c_{14}	≈ 0	–	–
K_V	36.46		
K_R	26.63		

Also listed is the Brilloiun zone results of Holuj et al. [12]. The last column shows the relative difference between the two results, calculated as the difference divided by the value of this work, times 100.

The strains applied to the unit cells of portlandite are all chosen to be ±0.01. Hooke's law in linear elasticity takes the form

$$\sigma_i = C_{ij} e_j \tag{2}$$

It may be shown that a small residual stress is taken into account by solving Hooke's law in the form

$$\left(\sigma_i - \sigma_i^r\right) = C_{ij}\left(e_j - e_j^r\right) \tag{3}$$

where σ_i^r is the residual stress, e_j^r is the residual strain and the term $(e_j - e_j^r)$ is the applied strain. The elastic constants are extracted from the stress–strain calculations by minimizing $|(\sigma_i - \sigma_i^r) - C_{ij}(e_j - e_j r)|$ using a least-square method, and taking into account the specific form of the stiffness matrix, Eq. (1).

The calculated elements of the stiffness matrix are listed in Table 1 together with the experimental values of Holuj et al. [12] obtained by Brillouin zone spectroscopy. The elastic constants are relatively large in the (001) plane both regarding tensile and transverse components (off-diagonal components), while the elastic constants are a factor 2.5–4 smaller when they include the c-axis. The values of the components are in reasonable agreement with the experimental results of Holuj et al. There is, however, a factor 4 in difference on the c_{13} component, which at present is unexplained. The remaining components differ by less than 25%. Because the relaxed lattice is very close to both the most recent X-ray study and the theoretical study by Baranek, there is good reason to believe that this work is more precise than the experiments by Holuj.

The Voigt (V) and Reuss (R) bounds [14,15] of the bulk modulus in terms of the stiffness constants c_{ij} for a trigonal lattice (which is identical to the relations of a hexagonal lattice) are given by

$$K_V = \frac{1}{9}\left[2(c_{11} + c_{12}) + c_{33} + 4c_{13}\right] \tag{4}$$

$$K_R = \frac{(c_{11} + c_{12})c_{33} - 2c_{13}^2}{c_{11} + c_{12} + 2c_{33} - 4c_{13}} \tag{5}$$

For portlandite, the bounds are found to be K_V=36.46 GPa and K_R=26.63 GPa, respectively. Experimetal values of the bulk modulus have been determined by Meade and Jeanloz [13] using X-ray diffraction measurements. They report a bulk modulus of 37.8±0.18 GPa. The VR bounds calculated from the DFT results are thus found to be just within the errors of the X-ray diffraction measurements.

Because crystal structures are usually anisotropic, so is the Young's moduli. Due to the symmetry of the trigonal lattice, there is only a very small variation in Young's modulus in the (001) plane. In the present case, c_{14} is zero and thus there is no variation at all. In Fig. 2, the variation of Young's modulus as function of the angle, θ, between the c-axis and the direction of deformation is shown. The global minimum value is 22.56 GPa and is found at θ=39.82°. A local maximum is present at parallel to c with the value 36.29 GPa. The global maximum is as expected present in the (001) plane with modulus 99.39 GPa.

4.3. Error estimate

The error sources due to the method of calculation arise in principle solely from the exchange functional, the pseudopotential, the k-point distribution and the plane wave energy cutoff used. Since the true values of the elastic moduli are not known, the magnitude of these errors is difficult to estimate. They may be assumed to be small, since the calculation is performed with a large number of k-points, a large number of plane waves and the use of spin-polarized calculations.

Errors due to lack of full convergence of the ionic forces and relaxation of the equilibrium state are estimated by calculating the elastic constants using nearly converged equilibrium states. The error due to this is less than 5%. Further errors are introduced due to the assumption of linearity of the elasticity. However, these contributions are very small compared to the errors due to the lack of full convergence of ionic forces and the residual stress and may thus be discarded.

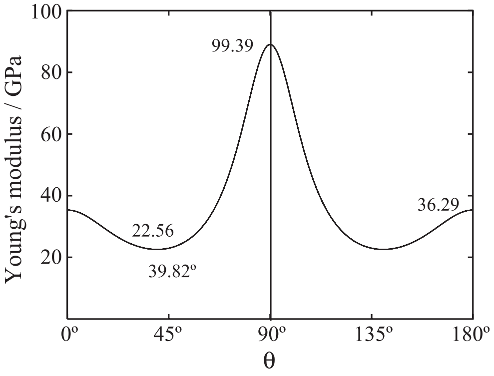

Fig. 2. The variation of Young's modulus with the angle between the direction of strain and the c-axis. As expected, the modulus is larger in directions perpendicular to the c-axis. There is only no variation in the (001) plane.

5. Conclusions

The equilibrium state of portlandite has been calculated by use of the plane wave pseudopotential method in density functional theory. The elastic stiffness constants were calculated by application of pure uniaxial and pure shear strains on the equilibrium state. Within the frame of the density functional method, the error in the elastic constants is estimated to be lower than 5%. Compared to experiments larger deviations are observed, probably due to impurities in the sample and due to the experimental method used. The calculated values follow the trend of the Brillouin zone spectroscopy experiments of Holuj et al. except the c_{13} value, where a large difference of factor 4 is present. Other components differ by about 25%. As expected from the structure and weak dispersive cohesive forces along the c-axis of portlandite, the Young's moduli are shown to have a very large directional dependency ranging from 22.56 to 99.39 GPa. The Voigt and Reuss bounds of the bulk modulus were calculated and shown to be within experimental values.

References

[1] Ph. Baranek, A. Lichanot, R. Orlando, R. Dovesi, Structural and vibrational properties of solid $Mg(OH)_2$ and $Ca(OH)_2$—performance of various hamiltonians, Chem. Phys. Lett. 340 (2001) 362–369.

[2] P. Hohenberg, W. Kohn, Inhomogeneous electron gas, Phys. Rev. 136 (1964) B864.

[3] W. Kohn, L.J. Sham, Self-consistent equations including exchange and correlation effects, Phys. Rev. 140 (1965) A1133.

[4] W. Koch, M.C. Holthausen, A Chemist's Introduction to Density Functional Theory, Wiley-VCH, Weinheim, Germany, 2001.

[5] DACAPO, The plane wave-pseudopotential program, version 2.6.1, CAMP, Department of Physics, Technical University of Denmark.

[6] J.P. Perdew, Y. Wang, Accurate and simple analytic representation of the electron–gas correlation energy, Phys. Rev., B 45 (23) (1992) 13244–13249.

[7] J.D. Bernal, H.D. Megaw, The function of hydrogen in intermolecular forces, Proc. R. Soc. A151 (1935) 384.

[8] H.E. Petch, H.D. Megaw, Crystal structure of brucite $MG(OH)_2$ and portlandite $Ca(OH)_2$ in relation to infrared absorption, J. Opt. Soc. Am. 44 (1954) 744–745.

[9] W.R. Busing, H.A. Levy, Neutron diffraction study of calcium hydroxide, J. Chem. Phys. 26 (1957) 563–568.

[10] H.J. Monkhorst, J.D. Pack, Special points for Brillouin-zone integrations, Phys. Rev., B 13 (12) (1976) 5188–5192.

[11] J.F. Nye, Physical Properties of Crystals, Oxford University Press, Oxford, 1985.

[12] F. Holuj, M. Drozdowski, M. Czajkowski, Brillouin spectrum of $Ca(OH)_2$, Solid State Commun. 56 (12) (1985) 1019–1021.

[13] C. Meade, R. Jeanloz, Static compression of $Ca(OH)_2$ at room temperature: observation of amorphization and equation of state measurements to 10.7 GPa, Geophys. Res. Lett. 17 (8) (1990) 1157–1160.

[14] P.J.M. Monteiro, The elastic moduli of calcium hydroxide, Cem. Concr. Res. 25 (8) (1995) 1605–1609.

[15] M.J.P. Musgrave, Crystal Acoustics, Holden-Day, San Francisco, 1970.